Thorium(IV) Diphosphazide Complexes: CO$_2$ Insertion into Th−C and Th−N Bonds

Tara K. K. Dickie and Paul G. Hayes*

Read Online

ACCESS | Metrics & More | Article Recommendations | Supporting Information

ABSTRACT: A thorium(IV) trialkyl complex, L_{PN3}Th-$(CH_2SiMe_3)_3$ (L_{PN3} = κ^5-2,5-$[(4-^iPrC_6H_4)N_3=P^iPr_2]_2N(C_4H_2)^{-}$), readily inserts carbon dioxide into the three Th−C bonds to afford L_{PN3}Th(κ^2-$O_2CCH_2SiMe_3$)$_3$ (**1**). A new thorium triamido complex, L_{PN3}Th(NHAd)$_3$ (**2**) was synthesized and inserts CO$_2$ into the Th−N bonds to form the tricarbamate species L_{PN3}Th(κ^2-O_2CNHAd)$_3$ (**3**). *In situ* heating experiments revealed that the supporting diphosphazide ligands in complexes **1** and **3** liberate 2 equiv of N$_2$ to form the corresponding diphosphinimine-supported complexes $L_{P=N}$Th(κ^2-$O_2CCH_2SiMe_3$)$_3$ (**4**, $L_{P=N}$ = κ^3-2,5-$[(4-^iPrC_6H_4)N=P^iPr_2]_2N(C_4H_2)^{-}$), and **5**, $L_{P=N}$Th(κ^2-O_2CNHAd)$_3$, respectively). Conversely, only one unit of N$_2$ was released from **2**, affording the asymmetric phosphazide/phosphinimine $L_{P=N/PN3}$Th(NHAd)$_3$ (**6**, $L_{P=N/PN3}$ = κ^3-2-$[(4-^iPrC_6H_4)N=P^iPr_2]$-5-$[(4-^iPrC_6H_4)N_3=P^iPr_2]N(C_4H_2)^{-}$). The addition of 3 equiv of either $ClSiMe_3$ or LiI to complex **1** generated L_{PN3}ThX$_3$ (X = Cl and I) and the carboxylate byproducts $Me_3SiO_2CCH_2SiMe_3$ and $LiO_2CCHSiMe_3$, respectively. Addition of $LiCH_2SiMe_3$ completed the stepwise synthetic cycle of thorium-mediated CO$_2$ functionalization.

xs CO$_2$

11-coordinate thorium

R = SiMe$_3$
R = NHAd
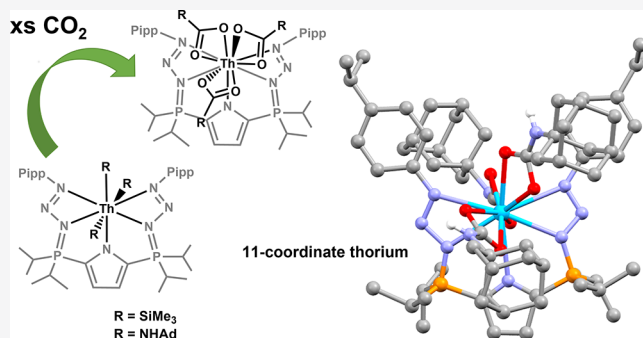
INTRODUCTION

Actinides have many properties that provide unique reactivity among the periodic table, including large ionic radii, high coordination numbers, and involvement of *f*-orbitals in bonding. These properties have inspired the quest for new actinide-mediated stoichiometric and catalytic reactions.[1] While small-molecule actinide chemistry is not as well-developed as that of the transition metals, the field is growing rapidly, especially with respect to the activation of carbon oxygenates (CO and CO$_2$).[2]

When exposed to CO$_2$, An(III) (An = Th and U) complexes can facilitate reductive coupling to form valuable C−C bond-containing products, such as oxalates.[3−6] While An(III) allows for intriguing small-molecule reactivity,[7−9] strong reducing agents, such as KC$_8$, are generally required for An(III) generation, and the desired reactivity may arrest upon metal oxidation, which tends to be highly facile. Conversely, An(IV) compounds primarily undergo CO$_2$ insertion into An−E bonds to produce carboxylates (E = C)[10,11] and carbamates (E = N).[12] A recent example of CO$_2$ insertion into hard−soft mismatched An−P bonds was published by Walensky and co-workers.[13] While stoichiometric functionalizations of CO$_2$ by Th and U species are known,[14−17] to our knowledge, catalytic conversion of CO$_2$ using an actinide complex has not yet been achieved.

The few reported examples of organoactinide-mediated CO$_2$ transformation have been achieved by utilizing XSiMe$_3$ (X = Cl

and I) to regenerate an An−X bond, along with concomitant formation of a silyl ester. The synthetic cycle can then be completed using a salt metathesis reaction to install an alkyl group at the metal center.[16,17] Recently, the Meyer group reported the anionic U(IV) oxo complex $[(2,6-Ad_2-4-Me-C_6H_2O)_3U(O)]^-$ (Ad = 1-adamantyl) which inserts CO$_2$ into U−O bonds to form carbonates.[16] The corresponding carbonates can be removed upon reaction with ISiMe$_3$. Reduction to U(III) using KC$_8$, subsequent oxidation to U(V) with N$_2$O, and a final KC$_8$ reduction back to the anionic U(IV) complex are required to complete the synthetic cycle. Additionally, Mazzanti and co-workers observed the formation of $[Th_2Cl(^{tBu}L_{salan})_2(\mu-\eta^1:\eta^1-O_2CCH_2SiMe_3)_2(\mu-\eta^1:\eta^2-O_2CCH_2SiMe_3)]$ ($^{tBu}L_{salan}$ = N,N'-bis(2-hydroxybenzyl-3,5-di*tert*-butyl)-1,2-dimethylaminomethane) from the dicarboxylate dimer in the presence of trace amounts of LiCl, cementing the theory that the driving force for removal of the carboxylate group from the metal center is the resultant Th−halide bond.[17]

We previously prepared actinide complexes supported by two ligand systems that contain the unusual phosphazide ($R_3P{=}N{-}N{=}N{-}R$) functionality (Figure 1). The "phosphazidosalen" U(IV) diphosphazide complex $L_{PN3salen}UCl_2$ ($L_{PN3salen} = \kappa^6\text{-}1,2\text{-}[N_3{=}PPh_2(2{-}O{-}C_6H_4)]_2C_6H_4$) features the first example of an actinide-stabilized phosphazide.[18] A monoanionic, pyrrole-based diphosphazide scaffold made it possible to isolate a rare trialkyl thorium complex, $L_{PN3}Th$-$(CH_2SiMe_3)_3$ ($L_{PN3} = \kappa^5\text{-}2,5\text{-}[(4\text{-}^iPrC_6H_4)N_3{=}P^iPr_2]_2N$-$(C_4H_2)^-$).[19] Notably, only a handful of other trialkyl thorium species are known,[20−22] several of which are active isoprene polymerization catalysts when combined with $[Ph_3C][B$-$(C_6F_5)_4]$.[20] A trialkyl complex such as $L_{PN3}Th(CH_2SiMe_3)_3$ could potentially demonstrate high catalytic functionalization of CO_2 because it has three sites where insertion can occur. Herein we describe the reactivity of $L_{PN3}Th(CH_2SiMe_3)_3$ toward CO_2, as well as the related reaction chemistry of the new triamide complex $L_{PN3}Th(NHAd)_3$ (**2**).

■ RESULTS AND DISCUSSION

CO_2 Insertion into Th−C and Th−N Bonds. A solution of the trialkyl complex $L_{PN3}Th(CH_2SiMe_3)_3$ in benzene-d_6, when placed under an atmosphere of CO_2, rapidly turns from bright orange to pale yellow upon vigorous mixing for a period of 5 min (Scheme 1). The $^{31}P\{^1H\}$ NMR spectrum exhibits a change from a single resonance at δ 59.4 ppm to two peaks at δ 54.7 and 55.4 ppm. The signal at δ 55.4 ppm subsequently converts slowly to δ 54.7 ppm, and after 24 h, the pale yellow color gives way to a colorless solution with only the peak at δ 54.7 ppm remaining. The identity of $L_{PN3}Th(\kappa^2$-$O_2CCH_2SiMe_3)_3$ (**1**), the product of CO_2 insertion into all three Th−C bonds, is supported by ^1H and $^{13}C\{^1H\}$ NMR data. Complete supplantation of the broad Th−CH_2SiMe_3 resonance at δ 0.15 ppm in the ^1H NMR spectrum by a sharp signal at δ 1.77 ppm integrating as 6H is consistent with three chemically equivalent Th−$O_2CCH_2SiMe_3$ groups. Furthermore, a peak in the $^{13}C\{^1H\}$ NMR spectrum at δ 188.3 ppm indicates the presence of a new carbonyl functionality. The complex giving rise to the $^{31}P\{^1H\}$ NMR chemical shift of δ 55.4 ppm is proposed to be the intermediate $L_{PN3}Th$-$(CH_2SiMe_3)(\kappa^2$-$O_2CCH_2SiMe_3)_2$, the product of only two CO_2 insertions.

Colorless X-ray quality crystals of complex **1** (Figure 2, left) were grown from a concentrated pentane solution at −35 °C. The large atomic displacement parameters for the entire structure imply a disordered crystal lattice. Notably, the structure appears to be an average of two different coordination isomers in the lattice, with one of the phosphazide groups positionally disordered. One isomer contains both phosphazide groups coordinated to thorium in a κ^2 fashion, and the other has one phosphazide bound only by
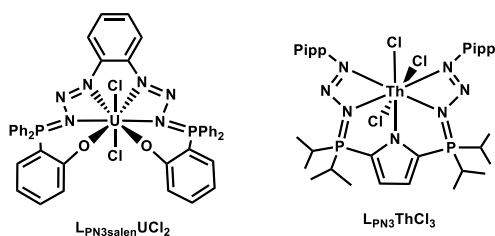
Scheme 1. Synthesis of Complexes 1−3
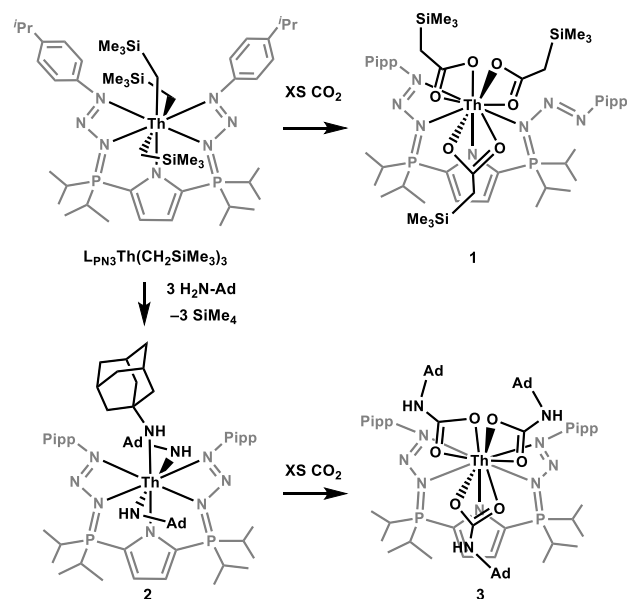
the α-nitrogen, resulting in an unusual *cis*-phosphazide (see Figure S23 for a disorder model showing an overlap of both components). The κ^1-*cis* coordination mode is the major component in the structure with an occupancy ratio of 71.9/28.1. *cis*-Coordinated phosphazides are far less common than their *trans*-counterparts.[23] In fact, this is the first example of a structurally characterized *cis*-phosphazide within this ligand framework; it features alternating N−N distances consistent with single- and double-bond character (N4−N5 = 1.365(18) Å, N5−N6 = 1.298(18) Å). In addition, the three $O_2CCH_2SiMe_3$ moieties are bound to thorium via a κ^2 interaction involving both oxygen atoms (Th−O_{ave} = 2.50 Å). As expected, delocalized C−O bonding is observed, giving rise to an average length of 1.25 Å.

Unlike the solid state, in benzene-d_6 solution, complex **1** exhibits C_{2v} symmetry on the NMR time scale (*vide supra*). Hence, the two different phosphazide coordination modes observed by X-ray crystallography are either a solid-state phenomenon or are rapidly exchanging at ambient temperature in solution. Although the κ^1-bonding mode may not dominate in solution, it is important to recognize that the system possesses coordinative isomerism which could prove valuable for accessing reactive intermediates.

Since Th−N bonds are prone to CO_2 insertion in the same manner as thorium alkyls, a thorium triamido complex was targeted for comparison purposes. When $L_{PN3}Th(CH_2SiMe_3)_3$ was mixed with 3 equiv of 1-adamantylamine in toluene, the orange solution immediately turned bright yellow. Upon washing the residue with pentane, small crystalline yellow needles were obtained. The ^1H NMR spectrum of the crystals in benzene-d_6 revealed multiple broad adamantyl signals between δ 1.50 and 2.50 ppm. Additionally, two broad N−H peaks at δ 3.58 and 2.87 ppm, integrating to 1H and 2H respectively, suggested the presence of three NH−adamantyl groups, two of which are equivalent on the NMR time scale. A lone singlet was observed in the $^{31}P\{^1H\}$ spectrum at δ 53.0 ppm.

X-ray diffraction experiments confirmed the identity of $L_{PN3}Th(NHAd)_3$ (**2**) indicated spectroscopically (Figure 3). Notably, both phosphazides are in the *trans*-orientation, unlike

Figure 1. Ligand systems that support actinide-stabilized phosphazides.
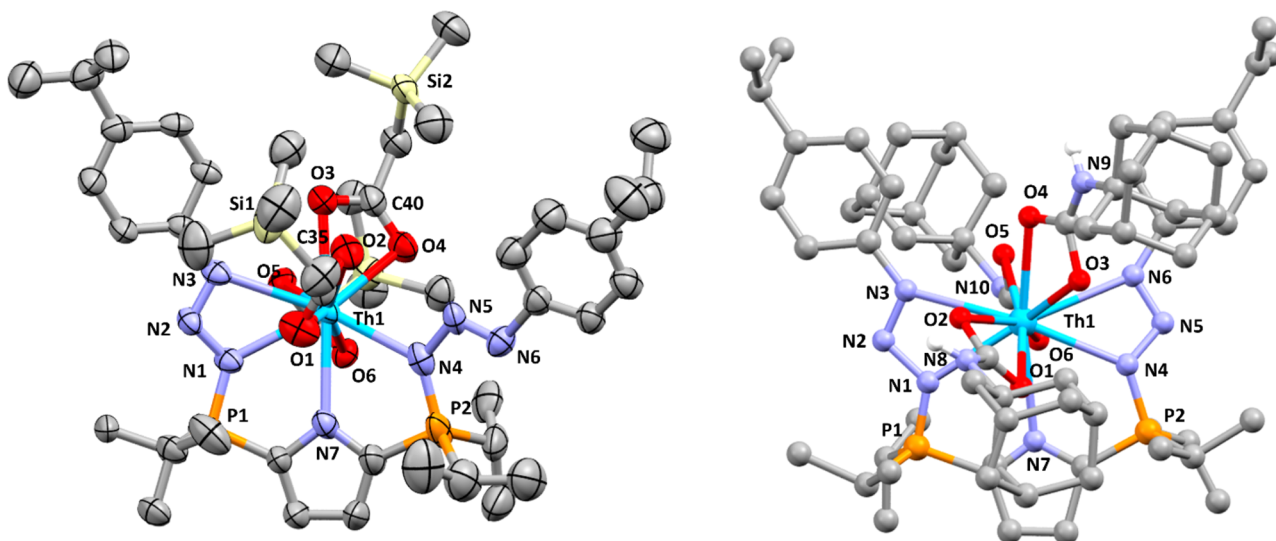
Figure 2. Left: X-ray crystal structure of complex **1** with thermal ellipsoids drawn at 30% probability. Hydrogens have been removed for clarity. Only the major component of the disorder model is shown. Selected bond distances (Å) and angles (deg): P1–N1 = 1.627(9), N1–N2 = 1.344(12), N2–N3 = 1.296(12), N7–Th1 = 2.652(10), Th1–N3 = 2.728(10), P2–N4 = 1.687(12), N4–N5 = 1.365(18), N4–N5B = 1.29(4), N5–N6 = 1.298(18), N5B–N6B = 1.26(7), Th1–O2 = 2.469(10), Th1–O1 = 2.445(10), Th1–O3 = 2.582(10), Th1–O4 = 2.518(8), O5–Th1 = 2.512(9), Th1–O6 = 2.504(7), C45–O6 = 1.273(13), C45–O5 = 1.238(13), O3–C40 = 1.239(16), C40–O4 = 1.294(17), C35–O2 = 1.277(19), C35–O1 = 1.202(18), N1–N2–N3 = 106.8(8), N4–N5–N6 = 105.9(13), O1–C35–O2 = 116.9(14), O3–C40–O4 = 123.3(14), O5–C45–O6 = 121.8(11), N7–Th1–O3 = 171.2(3). Right: Connectivity structure of complex **3**. Non-NH hydrogen atoms have been omitted for clarity.
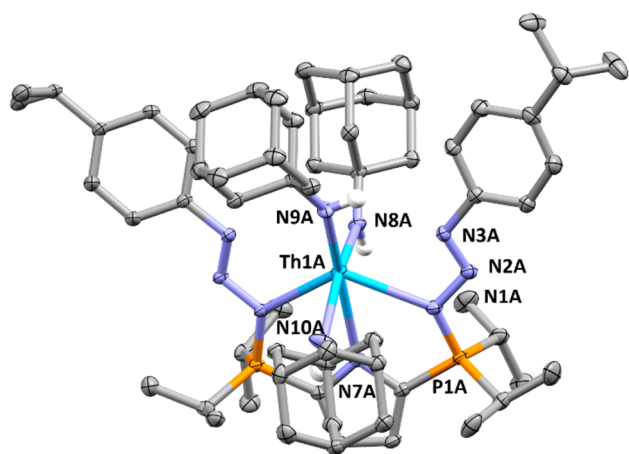
Figure 3. X-ray crystal structure of complex **2** with thermal ellipsoids drawn at 30% probability. Non-NH hydrogens have been removed for clarity. Only the major component of the disorder model is shown. Only one of the two independent molecules in the asymmetric unit is depicted. Selected bond distances (Å) and angles (deg): N1A–P1A = 1.642(3), N1A–N2A = 1.354(4), N2A–N3A = 1.268(4), P2A–N4A = 1.646(3), N4A–N5A = 1.352(4), N5A–N6A = 1.270(4), Th1A–N7A = 2.770(3), Th1A–N8A = 2.332(3), Th1A–N9A = 2.289(3), Th1A–N10A = 2.327(4), N1A–Th1A = 2.596(3), Th1A–N3A = 2.944(3), Th1A–N4A = 2.583(3), Th1A–N6A = 3.080(3), N1A–N2A–N3A = 108.8(3), N4A–N5A–N6A = 110.1(3), Th1A–N8A–C35A = 143.5(2), Th1A–N9A–C45A = 152.7(3), Th1A–N10A–C55A = 148.0(3), N9A–Th1A–N7A = 168.6(1), N10A–Th1A–N8A = 160.1(1).

that observed in complex **1**. Furthermore, the phosphazide γ-nitrogens reside quite far from the thorium center (Th1A–N3A = 2.944(3) Å, Th1A–N6A = 3.080(3) Å, cf. Th1–N3 = 2.73(1) Å in complex **1**), and accordingly, the nature of the Th–N$_\gamma$ interaction, if significant, is unclear. The N–N–N angles (N1A–N2A–N3A = 108.8(3)°, N4A–N5A–N6A =

110.1(3)°) within the *trans*-phosphazide moieties are comparable to those in both complex **1** (N1–N2–N3 = 106.8(8)°) and L$_{PN3}$Th(CH$_2$SiMe$_3$)$_3$ (N2–N3–N4 = 108.9(3)°).[19] The Th–N$_{adamantyl}$ distances range from 2.289(3) to 2.332(3) Å.

Upon addition of an atmosphere of CO$_2$ to a solution of bright yellow **2**, the color lightened immediately, implying the formation of L$_{PN3}$Th(κ^2-O$_2$CNHAd)$_3$ (**3**). A change in the ^{31}P{^{1}H} NMR spectrum (benzene-d_6) from δ 53.0 to 54.4 ppm was observed. The broad ^{1}H NMR NH signals in **2** (δ 3.58 and 2.87 ppm) collapsed into a single sharp peak at δ 3.99 ppm that integrates to 3H. Additionally, the number of adamantyl environments was reduced from five in **2** to three in complex **3**.

A low-quality connectivity X-ray structure of tricarbamate **3** revealed an exceedingly rare 11-coordinate thorium(IV) center,[24] with three κ^2-bound O$_2$CNHAd ligands (Figure 2, right). In contrast to complex **1**, both phosphazide groups are clearly coordinated to thorium via the α- and γ-nitrogen atoms. While thorium can access coordination numbers as high as 15, the most common for thorium(IV) is 8.[24,25] The vast majority of complexes that feature coordination numbers in excess of 10 are comprised of very small ligands, such as nitrates and oxides.[24] The geometry about thorium is best described as a distorted edge-coalesced icosahedron, with N1, N4, O1, and O6 forming the 4 vertices of the square plane, O2, N6, N3, O5, and O3 comprising the pentagonal plane, and O4 and N7 serving as capping atoms.

N$_2$ Loss from Phosphazide Ligands. Phosphazide groups stabilized by metal-coordination, H-bonding and sterically demanding groups are often heat-sensitive and will decompose with the loss of N$_2$ gas, forming the corresponding phosphinimine (P=N). For example, the previously reported phosphazidosalen ligand releases N$_2$ from the two ligand phosphazides. Specifically, L$_{PN3salen}$UCl$_2$ readily loses one

equivalent of N_2 at ambient temperature, but loss of the second N_2, to form the diphosphinimine complex $L_{P=NSalen}UCl_2$ ($L_{P=NSalen} = \kappa^4$-1,2-[N═PPh$_2$(2−O−C$_6$H$_4$)]$_2$C$_6$H$_4$), requires extensive heating at 155 °C.[18] The related pyrrole-based diphosphazide-supported complex $L_{PN3}Th(CH_2SiMe_3)_3$ decomposes into an intractable mixture after heating at 55 °C in hydrocarbon solvents for 24 h.[19] This decomposition is likely due to the highly reactive Th−C bonds, as well as the potential for cyclometalation of a *para*-isopropylphenyl (Pipp) C−H.

When a solution of **1** in benzene-d_6 was heated at 65 °C, a new dominant peak appeared in the $^{31}P\{^1H\}$ NMR spectrum at δ 48.7 ppm. In addition, signals at δ 57.0 and 48.3 ppm, due to low concentration intermediates, were also observed. After heating for 4 days, full conversion to $L_{P=N}Th(\kappa^2$-$O_2CCH_2SiMe_3)_3$ (**4**), the expected product of sequential loss of two molecules of N_2, was complete (Scheme 2). The resonances in the ^1H NMR spectrum attributed to complex **4** are shifted upfield from those in **1**, and the methylene peak is substantially broadened. Furthermore, the *ortho*-CH Pipp protons appear as a doublet of doublets ($^3J_{HH}$ = 8.4 Hz, $^4J_{HP}$ = 2.1 Hz), as the six bond separation between these atoms and the phosphazide phosphorus in **1** has been reduced to four.

Notably, complex **4** is inaccessible from the addition of CO_2 to a diphosphinimine complex. As previously established, the diphosphinimine trialkyl $L_{P=N}Th(CH_2SiMe_3)_3$ cannot be isolated as it rapidly undergoes cyclometallative decomposition to afford $L_{P=N}*Th(CH_2SiMe_3)_2$ ($L_{P=N}* = \kappa^4$-2-[(4-^{i}PrC$_6$H$_3$)-N═P^{i}Pr$_2$]-5-[(4-^{i}PrC$_6$H$_4$)N═P^{i}Pr$_2$]N(C$_4$H$_2$)$^{2-}$).[19] When the cyclometalated dialkyl complex $L_{P=N}*Th(CH_2SiMe_3)_2$ was exposed to an atmosphere of CO_2 in benzene-d_6 solution, immediate decomposition into an intractable mixture occurred. Intriguingly, cyclometalation of the diphosphinimine ligand in complex **4** appears to be wholly disfavored, presumably because such a process would generate the acid $HO_2CCH_2SiMe_3$.

Heating complex **3** in the same manner as that described above produces the diphosphinimine complex $L_{P=N}Th(\kappa^2$-$O_2CNHAd)_3$ (**5**), which exhibits a $^{31}P\{^1H\}$ NMR resonance at δ 47.2 ppm (Figure 4). Prior to complete conversion to complex **5**, signals attributed to an asymmetric intermediate were observed at δ 56.3 and 47.3 ppm. As in complex **4**, $^4J_{HP}$
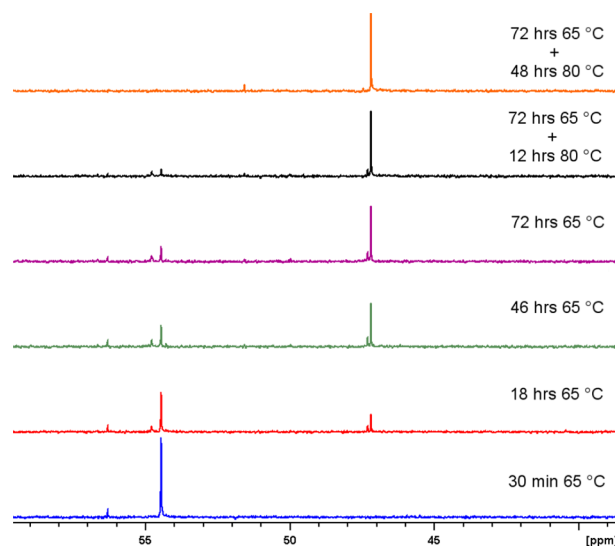
Figure 4. Stacked $^{31}P\{^1H\}$ NMR spectra of a sample of complex **3** in benzene-d_6 heated in a J. Young NMR tube.

coupling between the *ortho*-CH Pipp protons and the phosphinimine phosphorus atom was observed ($^3J_{HH}$ = 8.4 Hz, $^4J_{HP}$ = 2.0 Hz). Unfortunately, exhaustive attempts to isolate pure samples of complexes **4** and **5** were unsuccessful. Nonetheless, *in situ* NMR experiments unambiguously established liberation of N_2 gas afforded the expected phosphinimine-containing products.

Surprisingly, heating triamide **2** at 65 °C in benzene-d_6 for 72 h permitted isolation of the asymmetric phosphazide/phosphinimine complex $L_{P=N/PN3}Th(NHAd)_3$ (**6**, $L_{P=N/PN3}$ = κ^3-2-[(4-^{i}PrC$_6$H$_4$)N═P^{i}Pr$_2$]-5-[(4-^{i}PrC$_6$H$_4$)N$_3$═P^{i}Pr$_2$]N-(C$_4$H$_2$)$^-$). The $^{31}P\{^1H\}$ NMR spectrum of complex **6** contains two resonances of equal intensity at δ 49.7 and 46.1 ppm ($^4J_{PP}$ = 2.1 Hz). The number of ^1H environments has doubled relative to the triamide starting material, and the Pipp group bound to the phosphinimine nitrogen exhibits the familiar doublet of doublets common to complexes **4** and **5** ($^3J_{HH}$ = 8.3 Hz, $^4J_{HP}$ = 2.1 Hz). As in the ^1H NMR spectrum of **2**, one of the NH−adamantyl groups is distinct; two sharp NH signals integrate in a 1:2 ratio. It is not known why this asymmetric species is stable in solution at 65 °C, while the intermediates en route to complexes **4** and **5** are not. Presumably the difference in stability is due to steric protection exerted by the bulky adamantyl groups which raise the energy barrier for accessing the γ-nitrogen dechelated intermediate necessary for isomerization to the *cis*-phosphazide, and ultimately, loss of N_2.

X-ray diffraction experiments on complex **6** revealed a 7-coordinate distorted pentagonal bipyramidal thorium center (Figure 5). The intact *cis*-phosphazide is coordinated through both α- and γ-nitrogen atoms. The phosphinimine and pyrrole nitrogens, as well as one of the NH−Ad groups (N7), comprise the pentagonal plane. The N6−Th−N8 angle is nearly linear (171.3(3)°), and the N7 adamantyl group is positionally disordered across two sites. The three Th−N amide distances (Th1−N6 = 2.337(6) Å, Th1−N7B = 2.29(3) Å, Th1−N8 = 2.338(7) Å) are similar to those found in complex **2**. The phosphinimine P1═N1 distance of 1.610(9) Å is comparable to the coordinated phosphinimine in $L_{P=N}*Th(CH_2SiMe_3)_2$ (1.601(3) Å) and slightly shorter than that in $L_{P=N}ThCl_3$ (1.634(4) Å).[19]

Scheme 2. Synthesis of Complexes 4−6

R = SiMe (**1**)
R = NHAd (**3**)
R = SiMe (**4**)
R = NHAd (**5**)

2 **6**
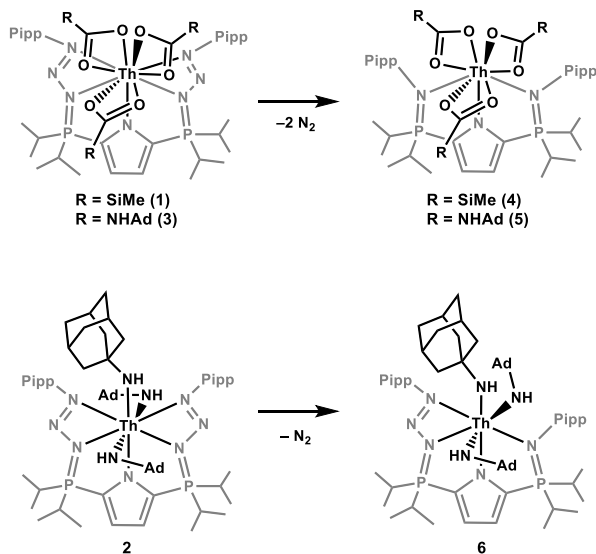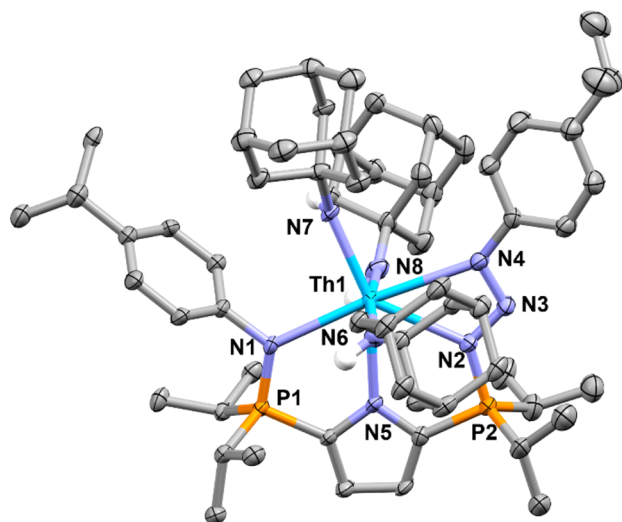
Figure 5. X-ray crystal structure of **6** with thermal ellipsoids drawn at 30% probability. Non-NH hydrogens have been removed for clarity. Only the major component of the disorder model is shown. Selected bond distances (Å) and angles (deg): P1−N1 = 1.610(9), P2−N2 = 1.64(1), N5−Th1 = 2.633(9), Th1−N6 = 2.337(6), Th1−N7B = 2.29(3), Th1−N8 = 2.338(7), Th1−N4 = 2.775(7), Th1−N2 = 2.59(1), Th1−N6−C33 = 152.7(6), Th1−N7B−C43B = 142(2), Th1−N8−C53 = 148.5(7), N2−N3−N4 = 108.0(8), N1−Th1−N4 = 174.6(2), N8−Th1−N6 = 171.3(3).

Reaction Chemistry of Complex 1. Preliminary experiments indicate that combination of **1** with excess H_2, $HSiEt_3$, $ZnMe_2$, or $B[N(SiMe_3)_2]_3$ in benzene-d_6 affords no reaction at ambient temperature. Meanwhile, addition of $AlMe_3$ resulted in rapid decomposition of the thorium complex.

Reaction of $ClSiMe_3$ with **1** produced the previously characterized compounds $L_{PN3}ThCl_3$ and $Me_3SiOCOCH_2SiMe_3$. When combined with the stepwise addition of alkyllithium, a closed synthetic cycle that transforms CO_2 and LiR into silyl esters is possible. Unfortunately, since $ClSiMe_3$ and $LiCH_2SiMe_3$ are incompatible reagents, this cycle requires stepwise stoichiometric addition for each transformation, making it impossible to complete the process catalytically.

When excess LiI was added to a solution of **1** in benzene-d_6 at ambient temperature, immediate yellow coloration occurred and a $^{31}P\{^1H\}$ signal at δ 57.0 ppm dominated the spectrum. This data, as well as that obtained from ^1H NMR spectroscopy, are consistent with $L_{PN3}ThI_3$. For example, the Th-κ^2-$O_2CCH_2SiMe_3$ methylene peak disappeared, and an extremely broad resonance (δ 0.00−0.70 ppm) attributed to $LiO_2CCH_2SiMe_3$ was observed. The success of this reaction implies that a catalytic transformation of $LiCH_2SiMe_3$ to $LiO_2CCH_2SiMe_3$ using LiI, CO_2, and $L_{PN3}ThCH_2SiMe_3$ is possible. However, $LiCH_2SiMe_3$ reacts with CO_2 under these conditions to form $LiO_2CCH_2SiMe_3$, rendering this actinide-catalyzed CO_2 transformation impractical.

CONCLUSIONS

The monoanionic diphosphazide ligand L_{PN3} stabilizes both trialkyl and triamido thorium(IV) complexes that undergo rapid and clean insertion of CO_2 into Th−C and Th−N bonds. The corresponding tricarboxylate and tricarbamate species are a result of the pentadentate diphosphazide ligand framework, as these types of complexes are not accessible using their P=N

ligand counterparts. The phosphazide moieties in this unique ligand system exhibit coordinative versatility (i.e., cis-, trans-, κ^1-, and κ^2-bonding modes), providing further evidence that phosphazides are underutilized functional groups in organometallic chemistry. Combination of $L_{PN3}Th(\kappa^2$-$O_2CCH_2SiMe_3)_3$ with $ClSiMe_3$ or LiI removes the carboxylate groups completing a synthetic CO_2 conversion cycle; however, further work is needed to achieve catalysis with an actinide complex.

ASSOCIATED CONTENT

Ⓢ Supporting Information

The Supporting Information is available free of charge at https://pubs.acs.org/doi/10.1021/acs.organomet.1c00638.

> Experimental details, synthesis and characterization of compounds, NMR and IR spectra, crystallographic details, and additional references (PDF)
> Cartesian coordinates (XYZ)

Accession Codes

CCDC 2108092−2108094 and 2122725 contain the supplementary crystallographic data for this paper. These data can be obtained free of charge via www.ccdc.cam.ac.uk/data_request/cif, or by emailing data_request@ccdc.cam.ac.uk, or by contacting The Cambridge Crystallographic Data Centre, 12 Union Road, Cambridge CB2 1EZ, UK; fax: +44 1223 336033.

AUTHOR INFORMATION

Corresponding Author

Paul G. Hayes − *Department of Chemistry and Biochemistry, University of Lethbridge, Lethbridge, Alberta T1K 3M4, Canada;* ⓘ orcid.org/0000-0001-6882-7897; Email: p.hayes@uleth.ca

Author

Tara K. K. Dickie − *Department of Chemistry and Biochemistry, University of Lethbridge, Lethbridge, Alberta T1K 3M4, Canada*

Complete contact information is available at:
https://pubs.acs.org/10.1021/acs.organomet.1c00638

Notes

The authors declare no competing financial interest.

REFERENCES

(1) Liu, H.; Ghatak, T.; Eisen, M. S. Organoactinides in catalytic transformations: scope, mechanisms and Quo Vadis. *Chem. Commun.* **2017**, *53*, 11278−11297.

(2) Arnold, P.; Turner, Z. R. Carbon oxygenate transformations by actinide compounds and catalysts. *Nat. Rev. Chem.* **2017**, *1*, 0002.

(3) Button, Z. E.; Higgins, J. A.; Suvova, M.; Cloke, F. G. N.; Roe, S. M. Mixed sandwich thorium complexes incorporating bis(tri-isopropylsilyl)cyclooctatetraenyl and pentamethylcyclopentadienyl

ligands: synthesis, structure and reactivity. *Dalton Trans.* **2015**, *44*, 2588−2596.

(4) Schmidt, A.-C.; Heinemann, F. W.; Kefalidis, C. E.; Maron, L.; Roesky, P. W.; Meyer, K. Activation of SO_2 and CO_2 by Trivalent Uranium Leading to Sulfite/Dithionite and Carbonate/Oxalate Complexes. *Chem. - Eur. J.* **2014**, *20*, 13501−13506.

(5) Tsoureas, N.; Castro, L.; Kilpatrick, A. F. R.; Cloke, F. G. N.; Maron, L. Controlling selectivity in the reductive activation of CO_2 by mixed sandwich uranium (iii) complexes. *Chem. Sci.* **2014**, *5*, 3777−3788.

(6) Formanuik, A.; Ortu, F.; Inman, C. J.; Kerridge, A.; Castro, L.; Maron, L.; Mills, D. P. Concomitant Carboxylate and Oxalate Formation From the Activation of CO_2 by a Thorium(III) Complex. *Chem. - Eur. J.* **2016**, *22*, 17976−17979.

(7) Boreen, M. A.; Arnold, J. The synthesis and versatile reducing power of low-valent uranium complexes. *Dalton Trans.* **2020**, *49*, 15124−15138.

(8) Odom, A. L.; Arnold, P. L.; Cummins, C. C. Heterodinuclear uranium/molybdenum dinitrogen complexes. *J. Am. Chem. Soc.* **1998**, *120*, 5836−5837.

(9) Summerscales, O. T.; Cloke, F. G. N.; Hitchcock, P. B.; Green, J. C.; Hazari, N. Reductive cyclotrimerization of carbon monoxide to the deltate dianion by an organometallic uranium complex. *Science* **2006**, *311*, 829−831.

(10) Moloy, K. G.; Marks, T. J. The insertion of carbon dioxide into actinide alkyl and hydride bonds. *Inorg. Chim. Acta* **1985**, *110*, 127−131.

(11) Higgins, J. A.; Cloke, F. G. N.; Roe, S. M. Synthesis and CO_2 Insertion Chemistry of Uranium(IV) Mixed-Sandwich Alkyl and Hydride Complexes. *Organometallics* **2013**, *32*, 5244−5252.

(12) Bagnall, K. W.; Yanir, E. Thorium (IV) and uranium (IV) carbamates. *J. Inorg. Nucl. Chem.* **1974**, *36*, 777−779.

(13) Tarlton, M. L.; Del Rosal, I.; Vilanova, S. P.; Kelley, S. P.; Maron, L.; Walensky, J. R. Comparative Insertion Reactivity of CO, CO_2, 'BuCN, and 'BuNC into Thorium− and Uranium−Phosphorus Bonds. *Organometallics* **2020**, *39*, 2152−2161.

(14) Matson, E. M.; Forrest, W. P.; Fanwick, P. E.; Bart, S. C. Functionalization of carbon dioxide and carbon disulfide using a stable uranium (III) alkyl complex. *J. Am. Chem. Soc.* **2011**, *133*, 4948−4954.

(15) Webster, C. L.; Ziller, J. W.; Evans, W. J. Synthesis and CO_2 Insertion Reactivity of Allyluranium Metallocene Complexes. *Organometallics* **2012**, *31*, 7191−7197.

(16) Waldschmidt, P.; Hoerger, C. J.; Riedhammer, J.; Heinemann, F. W.; Hauser, C. T.; Meyer, K. CO2 Activation with Formation of Uranium Carbonate Complexes in a Closed Synthetic Cycle. *Organometallics* **2020**, *39*, 1602−1611.

(17) Mora, E.; Maria, L.; Biswas, B.; Camp, C.; Santos, I. C.; Pécaut, J.; Cruz, A.; Carretas, J. M.; Marçalo, J.; Mazzanti, M. Diamine Bis(phenolate) as Supporting Ligands in Organoactinide(IV) Chemistry. Synthesis, Structural Characterization, and Reactivity of Stable Dialkyl Derivatives. *Organometallics* **2013**, *32*, 1409−1422.

(18) Dickie, T. K. K.; MacNeil, C. S.; Hayes, P. G. Consecutive N_2 loss from a uranium diphosphazide complex. *Dalton Trans.* **2020**, *49*, 578−582.

(19) Dickie, T. K. K.; Aborawi, A. A.; Hayes, P. G. Diphosphazide-Supported Trialkyl Thorium(IV) Complex. *Organometallics* **2020**, *39*, 2047−2052.

(20) Qin, G.; Cheng, J. Thorium(IV) trialkyl complexes of non-carbocyclic ligands as highly active isoprene polymerisation catalysts. *Dalton Trans.* **2019**, *48*, 11706−11714.

(21) Qin, G.; Wang, Y.; Shi, X.; Del Rosal, I.; Maron, L.; Cheng, J. Monomeric thorium dihydrido complexes: versatile precursors to actinide metallacycles. *Chem. Commun.* **2019**, *55*, 8560−8563.

(22) Chen, R.; Qin, G.; Li, S.; Edwards, A. J.; Piltz, R. O.; Del Rosal, I.; Maron, L.; Cui, D.; Cheng, J. Molecular Thorium Trihydrido Clusters Stabilized by Cyclopentadienyl Ligands. *Angew. Chem., Int. Ed.* **2020**, *59*, 11250−11255.

(23) Bebbington, M. W. P.; Bourissou, D. Stabilised phosphazides. *Coord. Chem. Rev.* **2009**, *253*, 1248−1261.

(24) Tutson, C. D.; Gorden, A. E. V. Thorium coordination: A comprehensive review based on coordination number. *Coord. Chem. Rev.* **2017**, *333*, 27−43.

(25) Daly, S.; Piccoli, P.; Schultz, A.; Todorova, T.; Gagliardi, L.; Girolami, G. Synthesis and Properties of a Fifteen-Coordinate Complex: The Thorium Aminodiboranate $[Th(H_3BNMe_2BH_3)_4]$. *Angew. Chem., Int. Ed.* **2010**, *49*, 3379−3381.